



This open access document is posted as a preprint in the Beilstein Archives at <https://doi.org/10.3762/bxiv.2022.64.v1> and is considered to be an early communication for feedback before peer review. Before citing this document, please check if a final, peer-reviewed version has been published.

This document is not formatted, has not undergone copyediting or typesetting, and may contain errors, unsubstantiated scientific claims or preliminary data.

**Preprint Title** Structure and local structural defects influence on the magnetic properties of cobalt nanofilms

**Authors** Alexander Vakhrushev, Aleksey Fedotov, Olesya Severyukhina and Anatolie Sidorenko

**Publication Date** 21 Jul 2022

**Article Type** Full Research Paper

**ORCID® IDs** Alexander Vakhrushev - <https://orcid.org/0000-0001-7901-8745>;  
Aleksey Fedotov - <https://orcid.org/0000-0002-0463-3089>; Anatolie Sidorenko - <https://orcid.org/0000-0001-7433-4140>

License and Terms: This document is copyright 2022 the Author(s); licensee Beilstein-Institut.

This is an open access work under the terms of the Creative Commons Attribution License (<https://creativecommons.org/licenses/by/4.0>). Please note that the reuse, redistribution and reproduction in particular requires that the author(s) and source are credited and that individual graphics may be subject to special legal provisions.

The license is subject to the Beilstein Archives terms and conditions: <https://www.beilstein-archives.org/xiv/terms>.

The definitive version of this work can be found at <https://doi.org/10.3762/bxiv.2022.64.v1>

# Structure and local structural defects influence on the magnetic properties of cobalt nanofilms

Alexander Vakhrushev\*<sup>1,3</sup>, Aleksey Fedotov<sup>1,2,3</sup>, Olesya Severyukhina<sup>1,2,3</sup> and Anatolie Sidorenko<sup>3</sup>

Address: <sup>1</sup>Modeling and Synthesis of Technological Structures Department, Institute of Mechanics, Udmurt Federal Research Center, Ural Division, Russian Academy of Sciences, Baramzinoy 34, Izhevsk 426067, Russia, <sup>2</sup>Nanotechnology and Microsystems Department, Kalashnikov Izhevsk State Technical University, Studencheskaya 7, Izhevsk 426069, Russia, <sup>3</sup>Orel State University named after I.S. Turgenev, Komsomolskaya Str. 95, 302026, Orel, Russia

Email:

Alexander Vakhrushev\* - Vakhrushev-a@yandex.ru

\* Corresponding author

## Abstract

The paper considers a mathematical model describing the time evolution of spin states and magnetic properties of a nanomaterial. We present the two variants of nanosystems simulations results. In the first variant, cobalt with a structure close to the hexagonal close-packed crystal lattice was considered. In the second case, the volume of the same size cobalt nanofilm formed in the previously obtained computational experiment of multilayer niobium-cobalt nanocomposite deposition

was investigated. For both simulations, it is obtained that, after pre-correction and significant jumps in the initial time moments, the change in spin temperature occurs in a small range of values near the average value. The system with a real structure has a less stable behavior of the spin temperature and a larger scatter of instantaneous values. For all cases of calculations for cobalt, the ferromagnetic character of the behavior is preserved. Defects in the structure and the local arrangement of the atoms can cause a deterioration of the magnetic macroscopic parameters, such as a decrease in the magnetization modulus.

## **Keywords**

Magnetic materials, nanofilms, nanocomposites, spintronics, molecular dynamics, LAMMPS

## **Introduction**

The analysis of phase transitions and related critical phenomena in condensed media is a complex, time-consuming, and often technologically high-cost process [1-3]. On the one hand, this is due to the need to use a comprehensive approach in theoretical studies, since the behavior of different phases is often described by different models or state equations [4]. Another reason is that phase transformation mechanisms originate at the nanoscale and atomic levels [5, 6], where observation and experiments require modern and expensive equipment. In this regard, precision experimental studies in critical regions are fraught with significant difficulties due to both temporal and spatial scales of objects behavior [4].

Despite the existing difficulties, the interest in the study of phase transitions is not decreasing. Evolutionary analysis of the structural transformations of substances

finds wide application in many areas of science and technology, including the physics of multicomponent systems. One promising application of multicomponent systems is developing phase-transition heat storage materials [7, 8], in which heat storage and accumulation occurs due to phase transformations. The functioning of such storage media is based on energy fluctuations in the process of crystallization or melting of the substance. In contrast to traditional media, thermal storage does not require sealing of the working volume during the change of aggregate states and is actively implemented as a highly efficient and energy-saving technology in the field of construction [9] and solar energy [10].

Phase transformations occupy an important position in the theories of superconductivity and ferromagnetic alloys. These theories actively consider composites with shape memory [11, 12]. Such composites are also called intelligent materials of the future [13] due to their unique functional properties and the possibility of restoring the original parameters under certain external conditions. Both thermodynamic conditions [14] and magnetoelectric fields [15] can act as external effects affecting the internal state and phase transitions of the samples. It has been shown in [11, 12, 16] that structural phase transitions in shape memory materials are in close relationship with external static and induction fields. Studying the role of magnetism on the structural features of composites opens up promising possibilities, since it allows predicting and creating new materials with controllable properties.

The idea of mutual correlation between the structure of matter and its magnetic properties is being developed in the field of spintronics. Modern computing devices face a number of difficulties during production, including those related to nanoscale computing elements arrangement on integrated circuits and their subsequent cooling during operation [17, 18]. The problems of excessive heat dissipation and performance improvement can be solved with the help of spintronics devices, which

are currently presented in a fairly wide variety of valuable effects: spin valves and valves in thin films and heterostructures [19, 20]; sensors based on the anomalous Hall effect [21]; spin injection and magnetism detection [22, 23]; giant magnetic resistance effects in data storage items and hard drives [24, 25]; ultrafast magneto-optical switches and optically induced ferromagnetics [26]. The discovery and implementation of topological insulators in Josephson contacts make spintronics devices excellent candidates for applications in quantum computing [27, 28] as well as in quantum cryptography [29].

The extensive influence of phase transitions and critical phenomena on the working properties of the samples testifies to the importance of a detailed study of structural transformations and possible stable states. Morphological analysis makes it possible to identify local defects in the crystal structure, facts of forming different-scale aggregates, which can further serve as causes of deterioration of the target material functional characteristics [30, 31]. Comprehensive studies in this area not only allow to establish the presence of heterogeneities and features of structure, but also to formulate the main laws of their origin and development.

This work is devoted to solving an important problem of revealing the relationship between the magnetic properties of multilayer nanocomposites and their structure. The problem of studying the influence of structure on the materials magnetic properties is not new and has been previously solved by other authors [4, 32-34]. For example, in [4], to describe the thermodynamic equilibrium and nonequilibrium properties of magnetic materials, a multiscale approach of mathematical modeling is used. This approach includes methods of first principles, spin models based on the stochastic Landau – Lifshitz – Hilbert equation and a submodel of micromagnetism, described by the Landau – Lifshitz – Bloch equation. The publication [32] is also devoted to the development of modeling methods in the field of materials phase

transitions, but with the help of classical and quantum Monte Carlo approaches. The main emphasis in the work is placed on studies of the statistical lattice model, including a high-precision calculation of the critical indices.

The intermetallic magnetic compound FeRh is discussed in [33]. In the considered material the thermodynamic first-order phase transition is observed near room temperature. Heating the material above the transition temperature changes its magnetic behavior from antiferromagnetic to ferromagnetic and is accompanied by a significant change in the crystal lattice structure and an increase in electrical conductivity. The material is promising for applied research and development of new spintronics devices, energy management sensors, and magnetic recording media.

Research focused on specific application devices based on the phase transition memory state is discussed in detail in [34]. Phase-transition memory technology is among the actively developing and promising technologies due to its ability to design devices of small size, high performance, durability, and cost-effectiveness. The authors of [34] review how the characteristics of phase transition memory combine with various potential applications, addressing some of the problems of this technology, including those related to cell design, negative structural features, and changes in the nanomaterial that can occur during fabrication.

Thus, the evaluation and elaboration of structural changes in a nanomaterial arising in the process of its technological production is an important task, often closely related to the composition of the sample in question. In this paper, we propose one of the mathematical models for investigating the relationship between the material structure and its magnetic properties. Mathematical modeling is used to estimate the influence of the disturbances in the atomic arrangement inside the crystal lattice, the appearance of destruction and fragmentation zones on the orientation of spins inside the material and the overall magnetization of the sample.

## **Description and conditions of the computational experiment**

The structure and magnetic properties of the nanomaterial were investigated in this work using a promising nanocomposite formed by alternating layers of cobalt and niobium. The proposed composite has potentially promising functional properties and can be used for magnetic systems with controlled effective energy exchange in Josephson contacts [35], which are successfully implemented in memory and information storage devices. A similar layered heterostructure, but with the addition of a thin platinum film, which is necessary for the generation of spin-orbit bonds, is also described in [36].

Comprehensive research on new promising materials is a complex multistage process. The general scheme of the problem-oriented analysis of a multilayer composite of niobium and cobalt is presented in Fig. 1. At the preparation of the conceptual model stage, the expected requirements to the main properties of the predicted material are formulated, a manufacturing method and an approximate composition are proposed on the basis of already existing technologies. The conceptual model for our study is based on a sample, the structure and composition of which is shown in the upper right part of Fig. 1.

At the next development stage it was required to simulate and systematize the technological processes of nanocomposite manufacturing, to establish the dependence of its structure and characteristics on the production parameters, to check the presence of target functional aspects, to determine the controllable properties, that is, those properties that are influenced and corrected in the process of manufacturing. The previously conducted studies considered the influence on the final properties of the sample of such technological parameters as the temperature of

the substrate on which the magnetron sputtering of nanofilms takes place, the intensity and deposition direction. The results of computational experiments are described in published papers [37-39].

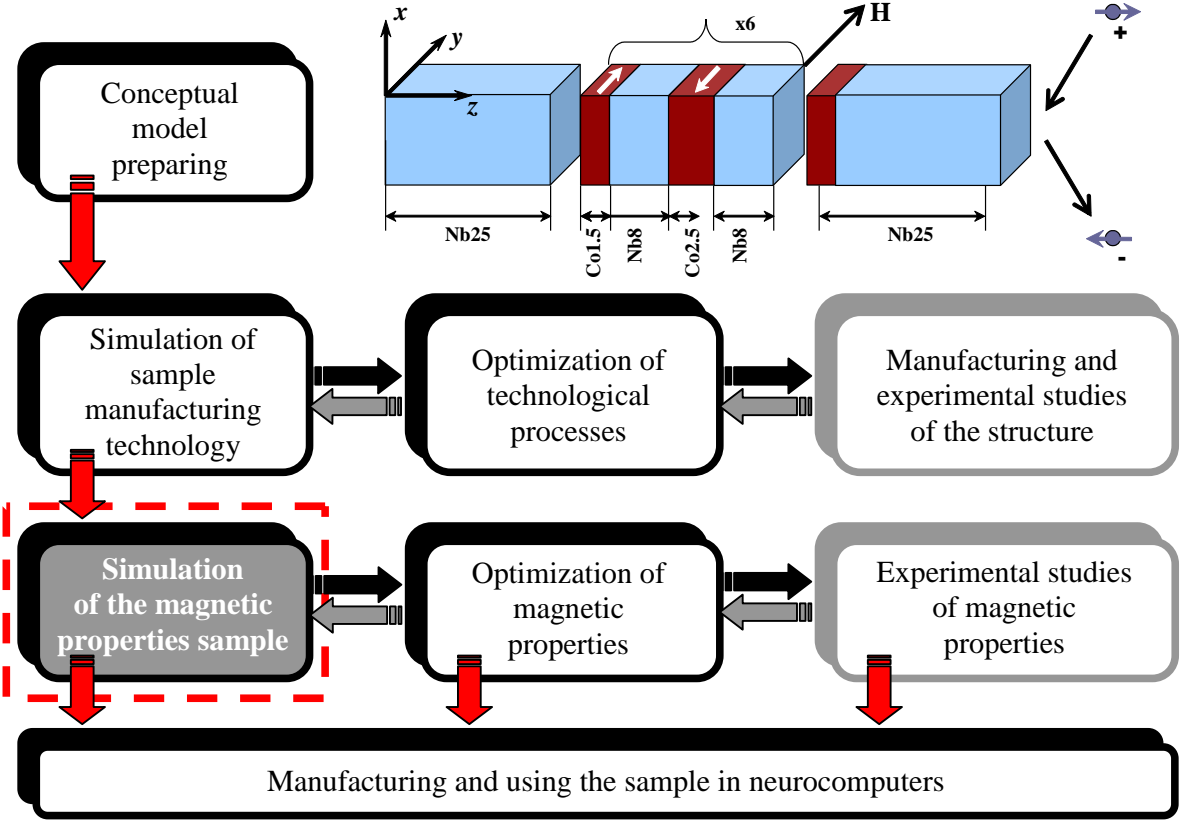


**Figure 1:** Problem statement for the complex study of cobalt and niobium heterostructures. The sketch of the Nb/Co spin-valve nanosystem was reproduced from [37] (© 2020 A. Vakhrushev et al., distributed under the terms of the Creative Commons Attribution License (<http://creativecommons.org/licenses/by/4.0>)).

The issue of optimizing the nanofilm interface involved the next stage of the sample study. The basic magnetic properties of the nanocomposite depend on the quality of the interface between the layers, so the problem of obtaining clearly separated contact layers is highly relevant. Using simulations, it was demonstrated that optimization of the nanofilm interface can be obtained either by introducing additional intermediate thin layers neutral to the original composition, such as aluminum oxide,

or by additional processing means, in particular mechanical alignment and intensive substrate cooling. The stage of experimental studies of the sample structure is necessary to identify the real structure of the nanocomposite and to compare the data with previously obtained simulation results.

The next stage of research is aimed at modeling the magnetic properties of the nanomaterial under study. This publication is devoted to exactly this stage of new promising heterostructure complex analysis task, so in Fig. 1 the block of modeling magnetic properties is highlighted by color and a dotted line. As noted earlier, the formed nanofilms have a non-ideal structure. Consequently, the influence of the real structure and local order of atoms on such parameters as magnetization, different types of energies, spin temperatures, and particle orientations remains open and of considerable practical interest.

The last two steps of the analysis, which include the optimization of magnetic properties and the experimental study of magnetic properties, are the subject of future research and are cited in the work for a complete understanding of the complex task of developing a new promising nanomaterial.

## **A mathematical model for studying the magnetic properties of nanomaterials**

When describing the magnetic properties of a nanosystem, the simultaneous equations of classical molecular dynamics are used, which are supplemented by considering the spin vectors  $s_i$  for each atom. The motion equation for atoms and spins is written in the form:

$$\frac{d\mathbf{r}_i}{dt} = \frac{\mathbf{p}_i}{m_i}, \quad (1)$$

$$\frac{d\mathbf{p}_i}{dt} = \sum_{i \neq j}^N \left[ -\frac{dU(|\mathbf{r}_{ij}|)}{d|\mathbf{r}_{ij}|} + \frac{dJ(|\mathbf{r}_{ij}|)}{d|\mathbf{r}_{ij}|} \mathbf{s}_i \cdot \mathbf{s}_j \right] \mathbf{e}_{ij}, \quad (2)$$

$$\frac{d\mathbf{s}_i}{dt} = \mathbf{f}_i \times \mathbf{s}_i, \quad (3)$$

where  $\mathbf{r}_i$  is the vector characterizing the position of the particle  $i$ ;  $\mathbf{s}_i, \mathbf{s}_j$  are the spin vectors;  $\mathbf{p}_i$  is the momentum;  $\mathbf{e}_{ij}$  is the unit vector along  $\mathbf{r}_{ij}$ ;  $\mathbf{f}_i$  is the analogue of the force applied to spin;  $U$  is the potential energy.

The general form of the expression for describing the total energy of magnetic systems can be written in the form:

$$H = H_z + H_{\text{ex}} + H_{\text{an}} + H_{\text{Neel}} + H_{\text{dm}} + H_{\text{me}} + H_{\text{di}}, \quad (4)$$

where the first two terms in the right-hand side are the Zeeman and exchange interactions, the next two terms describe magnetic anisotropy, followed by the terms responsible for the Dzialoshinsky – Moriya, magnetoelectric, and dipole interactions. The modeling consideration of different types of interactions depends on the structure of the systems considered, as well as on the problems that are solved in the simulation. Determination of parameters used to describe different types of interactions in modeling magnetic systems requires additional computational and experimental investigations. For this reason, the emphasis at this stage of research was placed on the pairwise anisotropy model of Neel.

The exchange interaction provides a natural relation between the spin and lattice degrees of freedom because of the function  $J$  dependence, which determines the intensity of the interaction, on the interatomic distance. It is noted in [40] that since  $J$  is usually only a radial function, the anisotropic effect cannot be modeled in this way. This excludes the most interesting and technologically attractive magnetostrictive properties of the materials, which are mainly direction-dependent and are due to the magnetocrystalline anisotropy energy of the materials. Since the source of the

magnetocrystalline anisotropy energy is the spin-orbit interaction of the atoms, it is necessary to take this interaction into account to perform accurate and realistic spin-lattice simulations.

The forms of magnetic anisotropy occurring in magnetics directly depend on the crystal lattice of the material under study. Magnetic anisotropy characterizes the change in the magnetic properties of ferromagnetic materials depending on the orientation of the spontaneous magnetization along the structural axes characteristic of the material. In a ferromagnetic crystal, depending on the orientation of the spontaneous magnetization, changes in internal energy are observed. Magnetic anisotropy occurs for several reasons, such as dipole-dipole interaction, temperature effects, sample parameters, or mechanical deformation. In the absence of external factors affecting the sample, the symmetry of the ferromagnetic crystal is governed by the value of the internal energy. This type of magnetic anisotropy is commonly referred to as magnetocrystalline, or magnetic crystallographic anisotropy. It is often caused by spin-orbit interaction (for magnetically ordered substances).

The dipole-dipole interaction does not make a significant contribution to the anisotropy energy and its value is insignificant. Only in a number of rare-earth metals the contribution of the dipole-dipole interaction can be significant because of the large magnetic moments of the atoms and small values of the crystal lattice parameters.

Approximations for modeling spin-orbit coupling have been proposed in [41, 42]. In particular, the functions proposed by Neel [41] for modeling the bulk magnetostriction and surface anisotropy in cobalt were used in [43]. The model proposed by Neel takes into account magnetocrystalline anisotropy in more complex forms as compared to uniaxial anisotropy. This model is used to describe magnetocrystalline anisotropy between pairs of magnetic spins:

$$\begin{aligned}
H_{\text{NeeI}} = & - \sum_{i,j=1,i \neq j}^N g_1(r_{ij}) \left( (\mathbf{e}_{ij} \cdot \mathbf{s}_i)(\mathbf{e}_{ij} \cdot \mathbf{s}_j) - \frac{\mathbf{s}_i \cdot \mathbf{s}_j}{3} \right) + \\
& + q_1(r_{ij}) \left( (\mathbf{e}_{ij} \cdot \mathbf{s}_i)^2 - \frac{\mathbf{s}_i \cdot \mathbf{s}_j}{3} \right) \left( (\mathbf{e}_{ij} \cdot \mathbf{s}_j)^2 - \frac{\mathbf{s}_i \cdot \mathbf{s}_j}{3} \right) + \\
& + q_2(r_{ij}) \left( (\mathbf{e}_{ij} \cdot \mathbf{s}_i)(\mathbf{e}_{ij} \cdot \mathbf{s}_j)^3 + (\mathbf{e}_{ij} \cdot \mathbf{s}_j)(\mathbf{e}_{ij} \cdot \mathbf{s}_i)^3 \right),
\end{aligned} \tag{5}$$

where the intensity of the dipole and quadrupole contributions are described using the functions  $g_1, q_1, q_2$ :

$$g_1(r_{ij}) = g(r_{ij}) + \frac{12}{35} q(r_{ij}), \tag{6}$$

$$q_1(r_{ij}) = \frac{9}{5} q(r_{ij}), \tag{7}$$

$$q_2(r_{ij}) = -\frac{2}{5} q(r_{ij}). \tag{8}$$

When modeling, it is convenient to describe the functions  $q(r_{ij})$  and  $g(r_{ij})$  with the Bethe – Slater curve:

$$f(r_{ij}) = 4\alpha \left( \frac{r_{ij}}{\delta} \right)^2 \left( 1 - \gamma \left( \frac{r_{ij}}{\delta} \right)^2 \right) e^{-\left( \frac{r_{ij}}{\delta} \right)^2} \Theta(R_c - r_{ij}), \tag{9}$$

where  $\alpha$  (in eV),  $\delta$  (in Å),  $\gamma$  (dimensionless value) are constant coefficients that depend on the structure of the sample under study;  $\Theta(R_c - r_{ij})$  is the Heaviside function. The coefficients  $\alpha, \delta, \gamma$  must be chosen so that the above function corresponds to the values of the magnetoelastic constant of the materials under consideration.

The following equation is used to calculate the spin temperature:

$$T_s = \frac{\hbar}{2k_B} \frac{\sum_{i=1}^N |\mathbf{s}_i \times \boldsymbol{\omega}_i|^2}{\sum_{i=1}^N \mathbf{s}_i \cdot \boldsymbol{\omega}_i}, \tag{10}$$

where  $s_i$  is vector representing magnetic spin of the particle,  $\omega_i$  is magnetic moment,  $\hbar$  is Planck constant. This approach to calculating spin temperature was proposed in [44].

The approach described in this paper and originally proposed by the authors [40] is implemented using direct simulation methods. At each moment of time, we do not know the assumed spin location, but we know its computed value, which is calculated on the basis of empirical parameters or other previously obtained data.. Therefore, an additional advantage is that systems of arbitrary size, including small ones, can be considered for calculating the magnetic properties based on the combined model of molecular dynamics and magnetization dynamics.

The technique used includes simulations of atomic magnetic spins associated with lattice vibrations. The dynamics of these magnetic spins can be used to simulate a wide range of phenomena related to magnetoelasticity or to study the influence of defects on the magnetic properties of materials.

## **Results of computational experiments and their discussion**

As computational experiments at the stage of modeling the technological processes of niobium and cobalt sample manufacturing showed, the structure of the formed layers is not ideal. Visually, noticeable crystallization zones are observed in the formed nanofilms, but also, along with them, there are areas of mixed structure, where the amorphous atomic structure most likely prevails. Quantitatively, the structure of nanofilms can be estimated, for example, by calculating the lattice ideality parameter [45]. This parameter is close to zero in ideal crystal lattices and has a

positive value where the structure of the material differs from the reference one, and the higher the value of the parameter, the higher the degree of discrepancy.

For the sample under study, the change in the ideality parameter, averaged over thin horizontal layers, is shown in Fig. 2. The legend to the figure provides information about the temperature of the substrate on which nanofilms were deposited in the computational experiments.

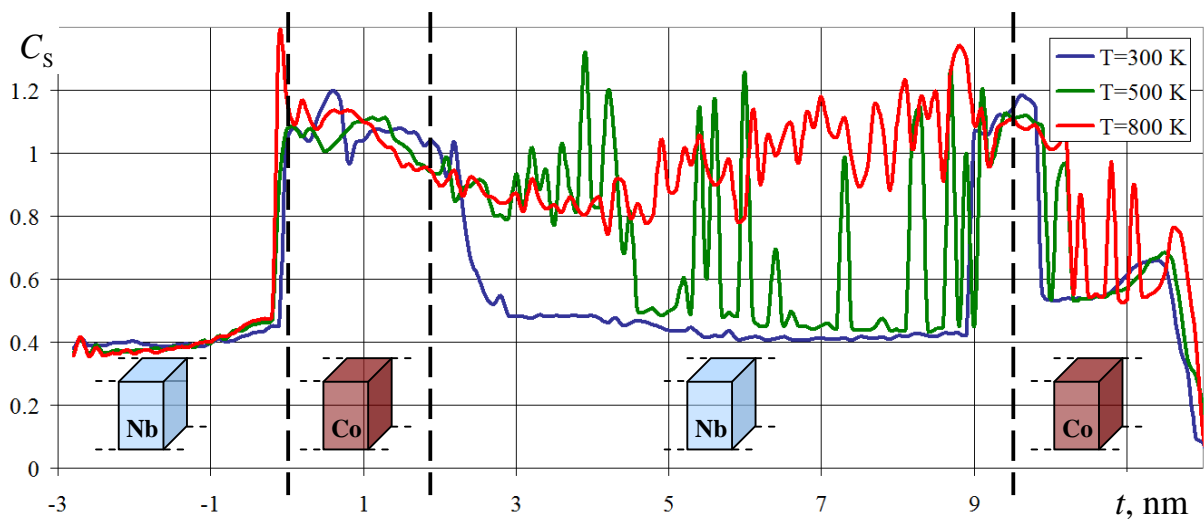


**Figure 2:** Variation of the average value of the crystal lattice ideality parameter in horizontal layers of niobium and cobalt nanocomposite. The schematic depictions of the Nb and Co layers were reproduced from [37] (© 2020 A. Vakhrushev et al., distributed under the terms of the Creative Commons Attribution License (<http://creativecommons.org/licenses/by/4.0>)).

Niobium is known as one of the actively used superconductors [46, 47] with a superconducting transition temperature for pure metal equal to 9.25 K. In superconductors, including niobium, due to the Meissner effect, the phenomenon of complete or partial ejection of the magnetic field from the material volume occurs [48, 49]. In the superconductivity mode, which is the mode of greatest interest for the magnetic behavior of the target film heterostructure, the absence of a

magnetic field is observed inside the metal, which is concentrated predominantly near the surface. For the reasons described above, niobium nanofilms were excluded from explicit consideration in computational experiments to investigate the magnetic properties of the spin nanocomposite, the appearance and structure of which are demonstrated in Fig. 3 (a).

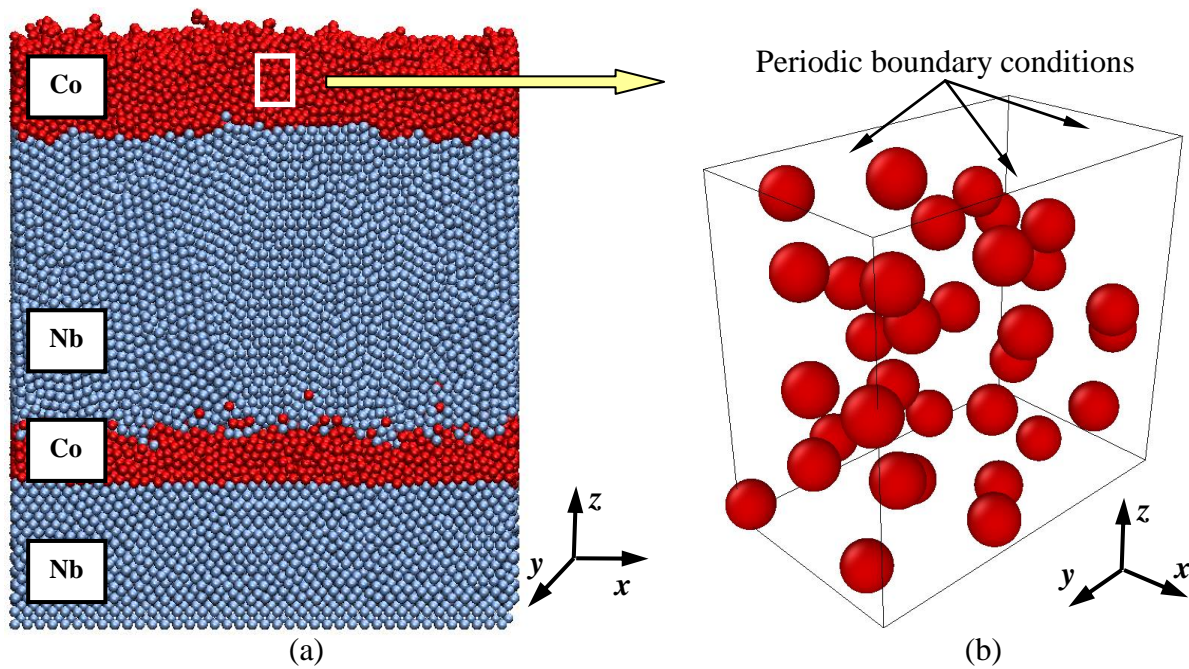


**Figure 3:** Multilayer nanocomposite of niobium and cobalt (a) formed in a computational experiment during deposition on a 300 K substrate and cut out a group of cobalt atoms to simulate magnetic properties (b). The image shown in (a) was adapted from [37] (© 2020 A. Vakhrushev et al., distributed under the terms of the Creative Commons Attribution License (<http://creativecommons.org/licenses/by/4.0>)).

In the task of investigating the magnetic properties of nanomaterials, the substrate temperature was set in the range of niobium nanofilm superconductivity mode operation at 5 K. In the problem of nanofilm deposition and structure formation, we considered three temperatures of the substrate on which the deposition took place: 300 K, 500 K, and 800 K. These temperatures are determined by the process

features of niobium and cobalt-based nanocomposite fabrication and can be seen in the legend shown in Fig. 2. In both tasks, magnetic property studies and studies of nanofilm deposition mechanisms, the substrate temperature was maintained using a Nose – Hoover thermostat.

Thus, at the initial stage of the magnetic characteristics studies, the spin behavior of only the cobalt atoms was analyzed for two variants of the calculations. In the first case, the cobalt atoms were located near the nodes of the hexagonal close-packed (HCP) crystal lattice, since this cobalt modification is the most stable at temperatures up to 700 K. The functional features of the nanocomposite involve its superconducting niobium nanolayers, so the simulation was performed at a nanosystem temperature of 5 K. For the first version of the computational experiment, a 2 x 2 x 2 unit crystal cell of HCP cobalt, bounded on all sides by periodic boundary conditions, was considered. The size of such a system is relatively small and is 0.5 nm x 0.87 nm x 0.82 nm.

For the second variant of the computational experiment, the real structure of cobalt nanofilms obtained earlier by simulating their deposition processes was considered. In order to preserve the structure of the cobalt nanofilm, a small volume was cut out in it, shown in Fig. 3 (a) as a white rectangle. This volume had strictly the same dimensions as the ideal HCP structure in the first computational experiment. A group of cobalt atoms with structural defects acquired as a result of film sputtering in an enlarged form is shown in Fig. 3 (b). Henceforward, to simplify the formulation, the nanosystem of cobalt atoms from the computational experiment with nanofilm deposition will be referred to as the real one.

The small size of the system in question was chosen for several reasons. First, the actual produced nanofilms in composites of cobalt and niobium have a small thickness, reaching 1-2 nm in some layers. Of practical interest are structural defects

and their influence on the magnetic properties exactly in thin films. Therefore, in our studies, a small volume in the cobalt nanofilm is cut out and the simulation results were compared to the corresponding volume with an ideal structure.

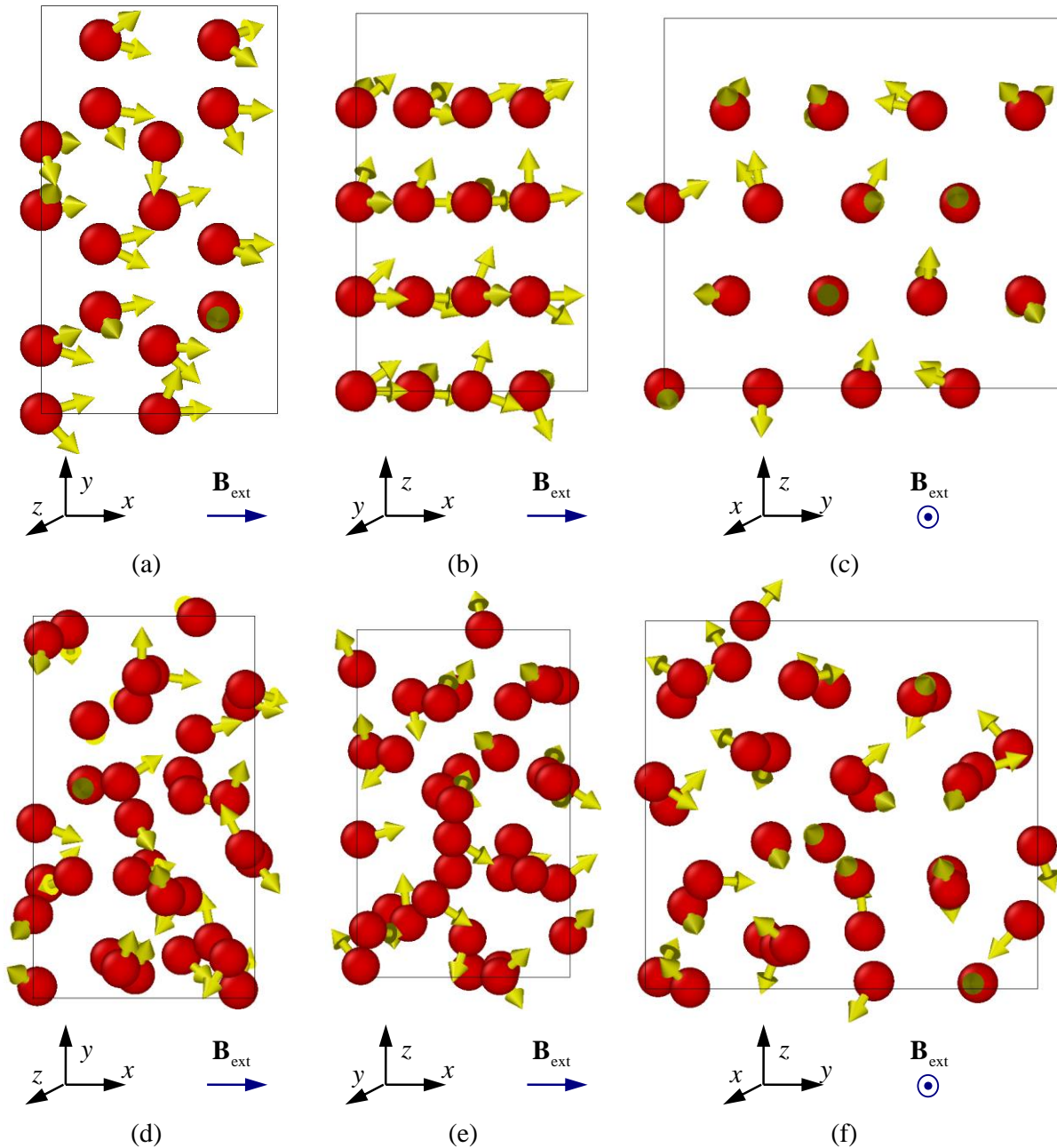


**Figure 4:** Spatial distribution of cobalt atoms spins for ideal crystal hexagonal close-packed lattice (a), (b), (c) and nanofilm structure (d), (e), (f) formed in the computational experiment at deposition on the substrate at 300 K, spin relaxation time 100 psec, external magnetic field value 1.0 T.

Second, the periodic boundary conditions used in molecular dynamics make it possible to balance the influence of direct boundary effects by symmetrically continuing identical computational volumes along those space directions where they are used, in our case along all three  $x$ ,  $y$ ,  $z$  directions. Third, the small computational cell in the work was used for clarity, so that the orientation of the individual atoms spins can be easily traced.

Subsequently, the selected two systems were exposed to an external magnetic field with induction  $\mathbf{B}_{\text{ext}} = 1.0 \text{ T}$  in the  $ox$  axis direction (along the nanofilm surface for the real structure variant) for a duration of 100 psec. The result of the spin distribution at the final moment is shown in Fig. 4. The time for which the spin distributions of the atoms in Fig. 4 corresponds to the value of 100 psec.

In order to catch the smallest changes in the spin behavior of the material and to take them into account in the research, an integration step of 0.1 fsec was chosen in the work. The normal and spin temperatures were maintained at the initial values of 5 K. The coordinates of the atoms changed insignificantly, which is associated with small thermal fluctuations and their linear velocities. As for the spin rearrangement, at the initial time moments corresponding to the interval of 0-5 psec, the change in the direction of the atoms' spins was active. At the initial moment of time, a chaotic distribution of spins was set for the atoms, regulated only by their initial spin temperature. Later, the direction of spins was influenced by the external magnetic field, as well as by their mutual arrangement and force behavior, which caused their reorientation.

Analysis of Fig. 4 shows that there are significant differences in the spin distributions of ideal crystalline hexagonal close-packed cobalt (letters (a), (b), (c)) and the nanofilm with structural defects formed as a result of the computational experiment (letters (d), (e), (f)). Crystalline cobalt is characterized by small changes in spin states

at finite time moments, with atoms spins being set in the direction of external magnetic field induction, i.e. ox axis. Nanofilms with structural defects and deviations from crystal lattice nodes are subject to greater randomness with respect to the direction of spins. The disordered orientation of spins is related to the enhanced influence of magnetic characteristics and forces of neighboring atoms. In the case of lattice distortions and defects in the material, zones of anomalies arise, which also bring about a stable magnetic state in the form of a local minimum of energy.

Internally, the behavior of atomic spins can be evaluated by calculating the spin temperature of the material. The spin temperature is equal to the normal temperature, but reflects the degrees of freedom of the atoms responsible for the magnetic energy fluxes. A graph of spin temperature variations for the two versions of ideal and real nanosystems under consideration is shown in Fig. 5.

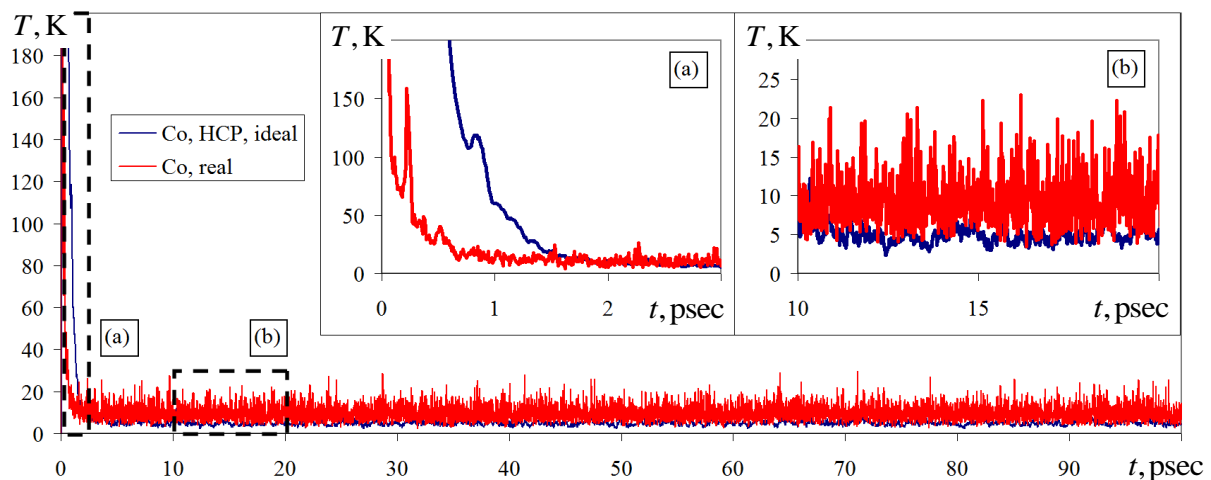


**Figure 5:** Changes in spin temperature in a constant external magnetic field of 1.0 T for ideal hexagonally close-packed cobalt and cobalt from the deposited nanofilm obtained in a computational experiment.

As can be seen from Fig. 5, at the initial moments of time 0-3 psec the spin temperature for both simulation variants is subject to considerable change. In the graph in Fig. 5, this time period is marked by the letter (a) and is shown in an

enlarged form. The jumps in the spin temperature transformation at 0-3 psec correspond to an active rearrangement of the spin directions of the atoms, which were unstable in the initial state due to the stochastic allocation. Subsequently, the spin temperature fluctuations decrease, its fluctuations occur near the thermostat target value of 5 K. For a time interval of 5-100 psec, the reorientation of spins is slow and mutually consistent, which is reflected in a small change in spin temperature. The system with a real structure has a less stable behavior of the spin temperature. The variation of this parameter in the range from 3 to 25 K indicates greater scatter and amplified oscillations of instantaneous values, compared to the case of an ideal structure.

Another macroscopic, but dependent on each atom, characteristic of the material is its magnetization. Magnetization determines the effect of partial or complete ordering of magnetic moments of a set of atoms under the influence of an external magnetic field, which allows using this value to evaluate the response of the nanocomposite to external factors, taking into account its structure and internal features. Dynamics of the vector modulus of the investigated sample during simulation for two variants of the investigated structure in a constant external magnetic field of 1.0 T is presented in Fig. 6.

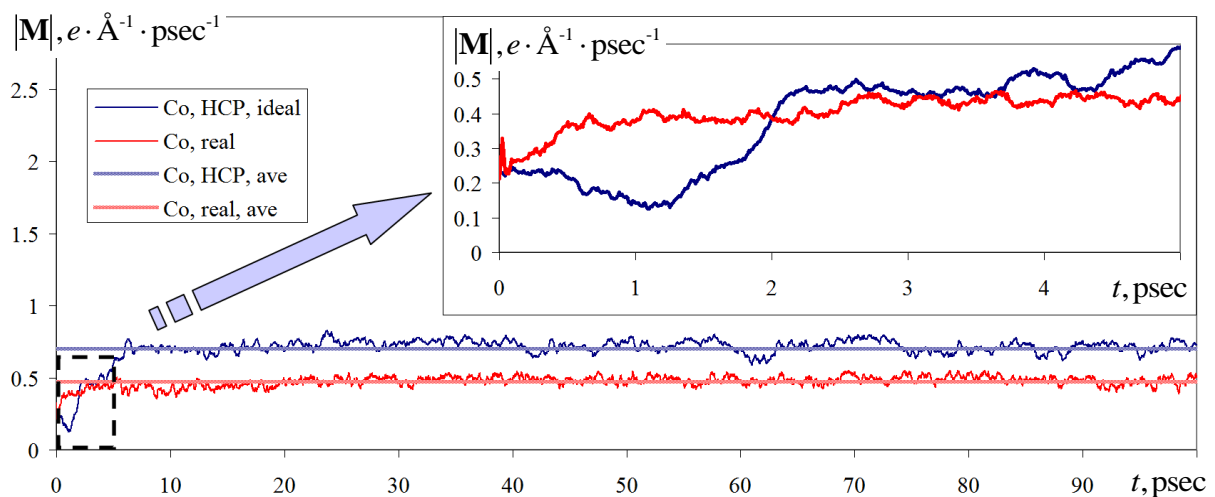


**Figure 6:** Changes in the magnetization vector modulus in a constant external magnetic field with an induction of 1.0 T for ideal hexagonally dense packed cobalt and cobalt from the deposited nanofilm obtained in the computational experiment.

The change in the modulus of the magnetization vector at the initial moments of time 0-7 psec is also characterized, like the spin temperature, by an increased variability. The rearrangement of the spin states of atoms does not allow us to find a stable energy state instantly, the movement to it is gradual. The length of the initial section of the magnetization graph with high volatility has a longer length compared to the same value for the spin temperature.

For a time interval of 7-100 psec, the magnetization modulus value is set near the mean value, which is  $0.7 e \cdot \text{\AA}^{-1} \cdot \text{psec}^{-1}$  for the case of an ideal crystal structure and  $0.47 e \cdot \text{\AA}^{-1} \cdot \text{psec}^{-1}$  for the real structure variant, where e is the notation of the electron charge. Such behavior of the nanomaterial is associated with the ordering of magnetic moments and is typical of ferromagnetics, one of which is cobalt [50, 51]. Thus, from the analysis of the graphs in Fig. 6 we can conclude that, despite the defects in the structure and the local arrangement of the atoms, cobalt retains its ferromagnetic character, but there may be a decrease or deterioration of the magnetic macroscopic parameters, such as the magnetization modulus.

## Conclusion

A mathematical model capable of reproducing the time evolution of spin states and magnetic properties of a nanomaterial, reflecting the response of an external magnetic field to the behavior of individual atoms, and taking into account the internal

structure and features of structural defects at the nanoscale when calculating the macroscopic magnetic characteristics of a physical body are proposed.

The study of the spatial distribution of cobalt atoms spins for an ideal crystalline hexagonal close-packed lattice and the structure of the nanofilm formed in a computational experiment during deposition on a substrate maintained at a constant temperature of 300 K shows that the spin directions are significantly dependent on the material structure. For an material structure external magnetic field with an induction of 1.0 T, a reorientation of spins along the external magnetic field is observed for crystalline ordered cobalt, whereas for cobalt from the nanofilm a more chaotic distribution of spins is characteristic, but also with a predominant direction parallel to the vector of induction of the external magnetic field.

In computational experiments for the ideal and real structure it is obtained that after preliminary adjustment and significant jumps in the initial moments of time, the change of spin temperature occurs in a small range of values near the average thermostat target value. The system with the real structure has a less stable behavior of the spin temperature and a larger scatter of instantaneous values, which may indicate a less energetically stable state of the nanomaterial.

Analysis of simulation results shows that for both variants of calculations, with ideal hexagonal close-packed and with real structure, ferromagnetic behavior is preserved for cobalt. Defects in the structure and local arrangement of atoms can be the cause of the deterioration of magnetic macroscopic parameters. For example, the magnetization modulus for the considered nanosystem in the case of the real structure decreased by 30-50 %.

The apparatus of mathematical modeling in this work serves as a predictive tool, allowing to correct technological processes of nanocomposite manufacturing and to reveal their weak points, for example, the influence of indistinctly separated

interfaces of nanofilms on the magnetic properties. Experimental studies on the subject of work are associated with a number of difficulties, the results on them are planned to be published in the following papers.

## Funding

The research was supported by the Russian Science Foundation project 20-62-47009, "Physical and Engineering Foundations of Non-Von Neumann Architecture Computers Based on Superconductor Spintronics".

## References

1. Markov, S. I.; Shurina, E. P.; Itkina, N. B. *Journal of Physics: Conference Series*, **2019**, 1333, No. 032052.
2. Hardtdegen, H.; Mikulics, M.; Riess, S.; Schuck, M.; Saltzmann, T.; Simon, U.; Longo, M. *Progress in crystal growth and characterization of material*, **2015**, 61, 27-45.
3. Pasupathy, A.; Velraj, R.; Seeniraj, R. V. *Renewable and Sustainable Energy Reviews*, **2008**, 12, 39-64.
4. Kazantseva, N.; Hinzke, D.; Nowak, U.; Chantrell, R. W.; Atxitia, U.; Chubykalo-Fesenko, O. *Physical Review B*, **2008**, 77, No. 184428.
5. Wang, Z.; Wei, J.; Morse, P.; Dash, J. G.; Vilches, O. E.; Cobden D. H. *Science*, **2010**, 327, 552-555.
6. Lin, Y. C.; Dumcenco, D. O.; Huang, Y. S.; Suenaga K. *Nature nanotechnology*, **2014**, 9, 391-396.
7. Chen, H.; Li, J.; Li, Y.; Cheng, X. *Journal of Alloys and Compounds*, **2020**, 829, No. 154574.

8. Wang, Y.; Tang, B.; Zhang, S. *Journal Of Materials Chemistry*, **2021**, *22*, 18145-18150.
9. Barrio, M.; Font, J.; Lopez, D. O.; Muntasell, J.; Tamarit, J. L. *Solar energy materials and solar cells*, **1992**, *27*, 127-133.
10. Bie, Y.; Li, M.; Malekian, R.; Chen, F.; Feng, Z.; Li, Z. *Applied Thermal Engineering*, **2018**, *135*, 218-227.
11. Oikawa, K.; Ota, T.; Ohmori, T.; Tanaka, Y.; Morito, H.; Fujita, A.; Kainuma, R.; Fukamichi, K.; Ishida, K. *Applied physics letters*, **2002**, *81*, 5201-5203.
12. Sutou, Y.; Imano, Y.; Koeda, N.; Omori, T.; Kainuma, R.; Ishida, K.; Oikawa, K. *Applied Physics Letters*, **2004**, *85*, 4358-4360.
13. Hager, M. D.; Bode, S.; Weber, C.; Schubert, U. S. *Progress in Polymer Science*, **2015**, *49*, 3-33.
14. Müller, I.; Seelecke, S. *Mathematical and computer modelling*, **2001**, *34*, 1307-1355.
15. Ullakko, K.; Huang, J. K.; Kantner, C.; O'handley, R. C.; Kokorin V. V. *Applied Physics Letters*, **1996**, *69*, 1966-1968.
16. Owerre, S. A. *Journal of Physics: Condensed Matter*, **2018**, *30*, No. 245803.
17. Paul, S.; Chatterjee, N.; Ghosal, P. *Journal of Systems Architecture*, **2019**, *98*, 271-288.
18. Najam, S.; Ahmed, J.; Masood, S.; Ahmed C. M. *IEEE Access*, **2019**, *7*, 25493-25505.
19. Zahnd, G.; Vila, L.; Pham, V. T.; Cosset-Cheneau, M.; Lim, W.; Brenac, A.; Laczkowski, P.; Marty, A.; Attané, J. P. *Physical Review B*, **2018**, *98*, No. 174414.
20. Zhou, T.; Mohanta, N.; Han, J. E.; Matos-Abiague, A.; Žutić, I. *Physical Review B*, **2019**, *99*, No. 134505.

21. Serlin, M.; Tschirhart, C. L.; Polshyn, H.; Zhang, Y.; Zhu, J.; Watanabe, K.; Taniguchi, T.; Balents, L.; Young, A. F. *Science*, **2020**, *367*, 900-903.
22. Das, K. S.; Liu, J.; van Wees, B. J.; Vera-Marun, I. J. *Nano letters*, **2018**, *18*, 5633-5639.
23. Gurram, M.; Omar, S.; van Wees, B.J. *2D Materials*, **2018**, *5*, No. 032004.
24. Abert, C. *The European Physical Journal B*, **2019**, *92*, 1-45.
25. Shen, R. L.; Zhong, J. *Journal of Engineering Tribology*, **2009**, *223*, 735-737.
26. Yamamoto, S.; Taguchi, M.; Someya, T.; Kubota, Y.; Ito, S.; Wadati, H.; Fujisawa, M.; Capotondi, F.; Pedersoli, E.; Manfreda, M.; Raimondi, L.; Kiskinova, M.; Fujii, J.; Moras, P.; Tsuyama, T.; Nakamura, T.; Kato, T.; Higashide, T.; Iwata, S.; Yamamoto, S.; Shin, S.; Matsuda, I. *Review of Scientific Instruments*, **2015**, *86*, No. 083901.
27. Meier, F.; Levy, J.; Loss, D. *Physical review letters*, **2003**, *90*, No. 047901.
28. Lehmann, J.; Gaita-Arino, A.; Coronado, E.; Loss, D. *Journal of materials chemistry*, **2009**, *19*, 1672-1677.
29. Kłobus, W.; Grudka, A.; Baumgartner, A.; Tomaszewski, D.; Schönenberger, C.; Martinek, J. *Physical Review B*, **2014**, *89*, No. 125404.
30. Amigo, N. *Molecular Simulation*, **2019**, *45*, 951-957.
31. Zong, B. Y.; Phuoc, N. N.; Wu, Y.; Ho, P.; Ma, F.; Han, G.; Yang, Y.; Li, Z.; He, S.; Wu, Y. *Chemelectrochem.*, **2015**, *2*, 1760-1767.
32. Kamilov, I. K.; Murtazaev, A. K.; Aliev, K. K. *Physics-Uspekhi*, **1999**, *42*, No. 689.
33. Lewis, L. H.; Marrows, C. H.; Langridge, S. *Journal of Physics D: Applied Physics*, **2016**, *49*, No. 323002.
34. Burr, G. W.; Breitwisch, M. J.; Franceschini, M.; Garetto, D.; Gopalakrishnan, K.; Jackson, B.; Kurdi, B.; Lam, C.; Lastras, L. A.; Padilla, A.; Rajendran, B.; Raoux, S.; Shenoy, R. S. *Journal of Vacuum Science & Technology B; Nanotechnology and*

*Microelectronics: Materials; Processing; Measurement; and Phenomena*, **2010**, 28, 223-262.

35. Klenov, N.; Khaydukov, Y.; Bakurskiy, S.; Morari, R.; Soloviev, I.; Boian, V.; Keller, T.; Kupriyanov, M. Sidorenko, A.; Keimer, B. *Beilstein J. Nanotechnol.*, **2019**, 10, 833-839.

36. Banerjee, N.; Ouassou, J. A.; Zhu, Y.; Stelmashenko, N. A.; Linder, J.; Blamire, M. G. *Physical Review B*, **2018**, 97, No. 184521.

37. Vakhrushev, A. V.; Fedotov, A. Yu; Boian, V.; Morari, R.; Sidorenko, A. *Beilstein J. Nanotechnol.*, **2020**, 11, 1776-1788.

38. Sidorenko, A. S.; Morari, R. A.; Boian, V.; Prepelitsa, A. A.; Antropov, E. I.; Savva, Yu. B.; Fedotov, A. Yu; Sevryukhina, O. Yu.; Vakhrushev, A. V. *Journal of Physics: Conference Series*, **2021**, 1758, No. 012037.

39. Vakhrushev, A. V.; Fedotov, A. Yu.; Sidorenko, A. S. *Key Engineering Materials*, **2021**, 888, 57-65.

40. Tranchida, J.; Plimpton, S. J.; Thibaudeau, P.; Thompson, A. P. *Journal of Computational Physics*, **2018**, 372, 406-425.

41. Beaujouan, D.; Thibaudeau, P.; Barreteau, C. *Physical Review B*, **2012**, 86, No. 174409.

42. Perera, D.; Eisenbach, M.; Nicholson, D. M.; Stocks, G. M.; Landau, D. P. *Physical Review B*, **2016**, 93, No. 060402.

43. Neel, L. *Journal de Physique et le Radium*, **1954**, 15, 376-378.

44. Nurdin, W. B.; Schotte, K. D. *Physical Review E*, **2000**, 61, 3579-3582.

45. Kelchner, C. L.; Plimpton, S. J.; Hamilton J. C. *Phys. Rev. B*, **1998**, 58, 11085-11088.

46. Finmore, D. K.; Stromberg, T. F.; Swenson C. A. *Physical Review*, **1966**, 149, 231-243.

47. Casalbuoni, S.; Knabbe, E.; Kötzler, J.; Lilje, L.; Von Sawilski, L.; Schmueser, P.; Steffen B. *Nuclear Instruments and Methods in Physics Research Section A: Accelerators; Spectrometers; Detectors and Associated Equipment*, **2005**, *538*, 45-64.
48. Aull, S.; Kugeler, O.; Knobloch, J. *Physical Review Special Topics-Accelerators and Beams*, **2012**, *15*, No. 062001.
49. Thompson, D. J.; Minhaj, M. S. M.; Wenger, L. E.; Chen, J. T. *Physical review letters*, **1995**, *75*, 529-532.
50. Moragues-Canovás, M.; Talbot-Eckelaers, C. E.; Catala, L.; Lloret, F.; Wernsdorfer, W.; Brechin, E.K.; Mallah, T. *Inorganic chemistry*, **2006**, *45*, 7038-7040.
51. Batallan, F.; Rosenman, I.; Sommers, C. B. *Physical Review B*, **1975**, *11*, 545-557.